MICROMECHANICAL RESONANT DISPLACEMENT GAIN STAGES

B. Kim, Y. Lin, W.-L. Huang, M. Akgul, W.-C. Li, Z. Ren, C. T.-C. Nguyen*
University of California, Berkeley, Department of EECS, Berkeley, California, USA
*Now at RF Micro Devices, Greensboro, North Carolina, USA

ABSTRACT

Micromechanical resonant displacement gain stages have been demonstrated that employ directionally engineered stiffnesses in resonant structures to effect displacement amplification from a driven input axis to an output axis. Specifically, the introduction of slots along the output axis of a 53-MHz wine-glass mode disk resonator structure realizes a single gain stage with a measured input-to-output displacement amplification of 3.08x. Multiple such mechanical displacement gain stages can then be cascaded in series via half-wavelength beam couplers to achieve multiplicative gain factors; e.g., two cascaded gain stages achieve a total measured gain of 7.94x. The devices have also been operated as resonant switches, where displacement gain allows impact switching via actuation voltages of only 400mV, which is 6x smaller than for previous resoswitches without displacement gain. The availability of such high frequency displacement gain strategies for resonant switches may soon allow purely mechanical periodic switching applications (such as power amplifiers and power converters) with much higher efficiencies than current transistor-based versions.

INTRODUCTION

Micromechanical switches operating at radio frequencies (RF) have exhibited superior performance over transistor-based counterparts in insertion loss, isolation, and power handling capability [1]. In particular, the small input capacitance of MEMS switches offers switch figure of merits (FOM's) several orders better than transistor counterparts, which could substantially enhance the efficiency of periodic switch applications, such as power amplifiers and converters. However, the majority of MEMS switches demonstrated so far still suffer from slow switching speeds, large actuation voltages, and poor long-term reliability. These unsolved issues greatly limit the use of these devices in RF applications, e.g., phased-array antennas, and outright prevents them from addressing higher volume switched-mode power amplifier or power converter applications.

To address these issues, the micromechanical resoswitch was recently introduced in [2, 3]. As shown in Figure 1a, this device comprises a wine-glass mode disk resonator similar to those previously used for oscillator and filter applications [4, 5], but now driven harder so that its conductive disk structure impacts surrounding electrodes. This then electrically shorts the disk and electrodes, thereby effecting periodic on/off switching at the disk's resonance frequency. By harnessing the resonance and nonlinear dynamical properties of their mechanical structures, resoswitches achieve significantly lower actuation voltage (~2.5V), much faster switching speed (rise time ~4ns), and substantially longer cycle lifetimes (>16.5 trillion cycles), than conventional MEMS switch counterparts, making them far more suitable for applications where periodic switching is needed [2, 3].

The resoswitch structure of [2, 3], however, was only a demonstration vehicle, with numerous imperfections. Aside from its polysilicon (rather than metal) construction, it suffered from the fact that during vibration its structure impacts not only the output (switch) electrodes, but also the input (control) electrodes, and this input-impacting behavior greatly limits intended applications, such as the Class-E power amplifier illustrated in Figure 1b. The reason for impacting along both axes is simply that the tiny lateral electrode-to-disk gaps required for capacitive transduction of the device were formed not by lithography, but by a sacrificial spacer film deposition that sets all gap spacings, input and output, to one value (less than 100nm) [3, 4]. One obvious remedy to this problem is to use multiple sacrificial sidewall layers with appropriate masking steps to achieve different gap spacings along the input axis and the output axis. However, this approach entails a more complicated process flow, and thus, might sacrifice production yield and cost.

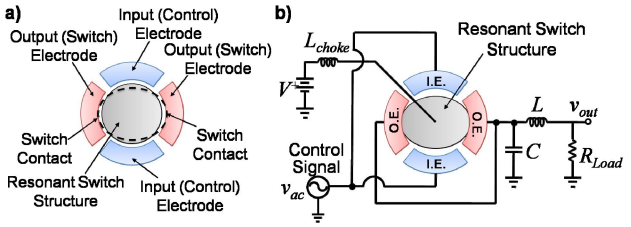

Figure 1: a) Schematic of a wine-glass disk "resoswitch" structure. When the structure resonates in the mode shape shown, it impacts select electrodes, effectively closing the switch. b) Example circuit diagram of a Class-E power amplifier utilizing this resoswitch.

This work offers a much better solution that dispenses with the need for process modification and rather utilizes a design-centric approach to effect displacement amplification in the switch structure. In particular, via directional stiffness engineering, the resonator structure generates larger displacements along its output axis than its input, so that impact occurs only at the output electrodes. This solves a major issue with the resoswitch of Figure 1a and makes it more suitable for mechanical power converters and amplifier applications.

DISPLACEMENT GAIN STAGE DESIGNS

Disk Resonators with Slots

Figure 2 presents overhead schematics and ANSYS-simulated mode shapes for (a) a conventional wine-glass mode disk resonator; and (b) a new slotted disk resonator design that provides displacement amplification between orthogonal axes. The conventional disk resonator (Figure 2a) exhibits its maximum displacement along two orthogonal axes (*a1-axis* and *a2-axis*), where the magnitude of the displacement along these two axes is identical. In contrast, the new resonator design (Figure 2b) introduces slots along the *b2-axis*, which then reduces the stiffness along this axis relative to that along the *b1-axis*. As a result, at resonance, the displacement along the *b2-axis* becomes much larger than that along the *b1-axis,* effecting dis-

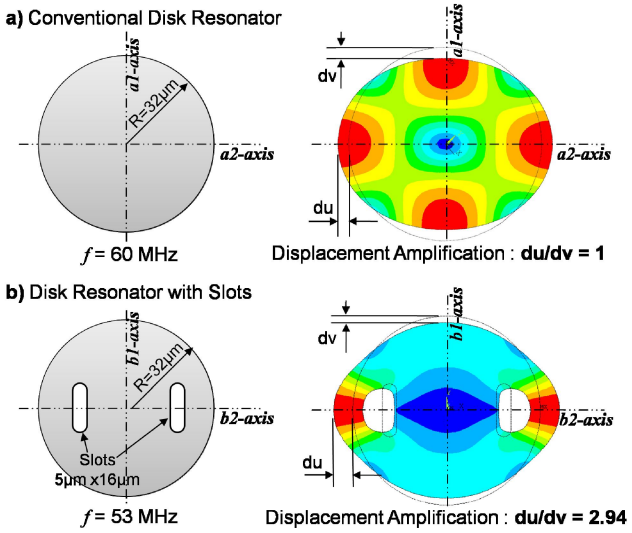

Figure 2: Design shapes and ANSYS FEA simulated mode shapes (wine-glass mode) of a) a conventional disk resonator and b) a disk resonator with slots. At resonance, the conventional disk has identical displacement along the a1-axis and the a2-axis, while the displacement along the slotted axis (b2-axis) is larger by 2.94x than the orthogonal axis (b1-axis) in the case of the disk resonator with slots.

placement amplification. ANSYS finite element simulation in fact predicts that the displacement along the slotted *b2-axis* is 2.94x larger than the displacement along the orthogonal *b1-axis*.

Figure 3 compares curves of normalized radial displacement ζ versus angular location along the perimeter θ for the two disk resonator designs operating in their wine-glass modes. Near the vertical axis ($0<\theta<45°$), both disk resonators exhibit similar mode shapes. The conventional disk resonator has a symmetric mode shape along the quasi-node point at θ=45°. However, the relative radial displacement of the slotted disk resonator increases rapidly for angles past the nodal point and finally becomes 2.94x greater along the horizontal axis at θ=90° than along the vertical axis at θ=0°.

Resonant Displacement Gain Stage Cascade

For further displacement amplification, displacement gain stages (disk resonators with slots) can be cascaded in series via beam couplers. These beam couplers become

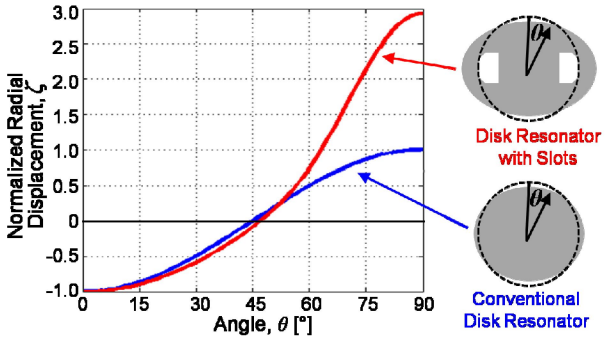

Figure 3: Mode shape comparison between a conventional disk resonator and the resonant gain stage. Here, radial displacements are normalized to the maximum displacement of the conventional disk resonator.

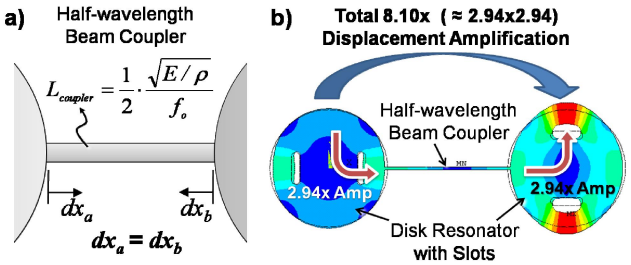

Figure 4: a) The motions of two resonators connected by a beam coupler are synchronized when the beam length is half-wavelength. b) ANSYS FEA simulation predicts multiplication of displacement gains when two gain stages are series cascaded, yielding 8.10x total displacement gain.

most efficient when their dimensions correspond to extensional-mode half-wavelengths at the disk resonance frequency, at which point their dynamic stiffnesses become virtually infinite [6]. As a result, the motion of one resonator is effectively transferred to the next, as shown in Figure 4a [5]. In effect, coupling two slotted resonator displacement gain stages using a half-wavelength beam coupler, attaching to one at its small displacement point and the other at its large displacement point, multiplies the gains of each stage, yielding a much higher total gain. ANSYS finite element simulations for the two slotted disk cascade shown in Figure 4b predict 8.10x of total displacement amplification, further attesting to gain multiplication.

EXPERIMENTAL VERIFICATION

Fabrication

For experimental verification, micromechanical resonant gain stages were fabricated via a small lateral-gap

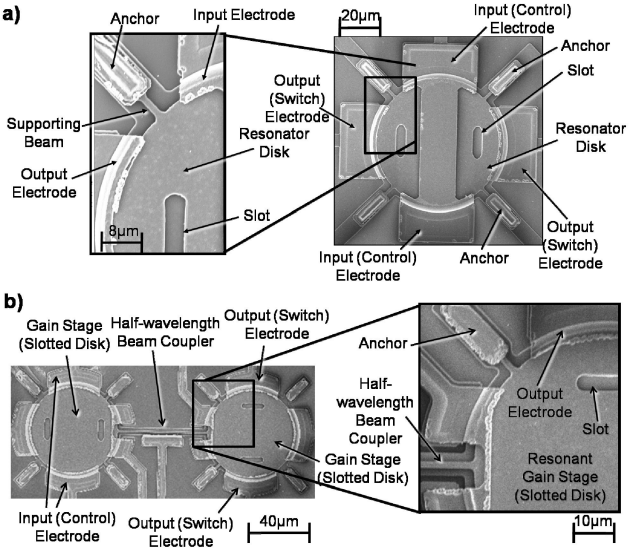

Figure 5: SEM's of fabricated micromechanical resonant gain stages. a) A single gain stage (disk resonator with sots). Slots (5μm x 16μm) were etched into a polysilicon disk resonator to realize the key amplifying features. b) A two slotted-disk resonator cascade, coupled via a half-wavelength beam coupler for further displacement amplification. The coupling beam connects a point along the slotted axis of the first resonator to a point along the un-slotted axis of the second to effect multiplication of gains.

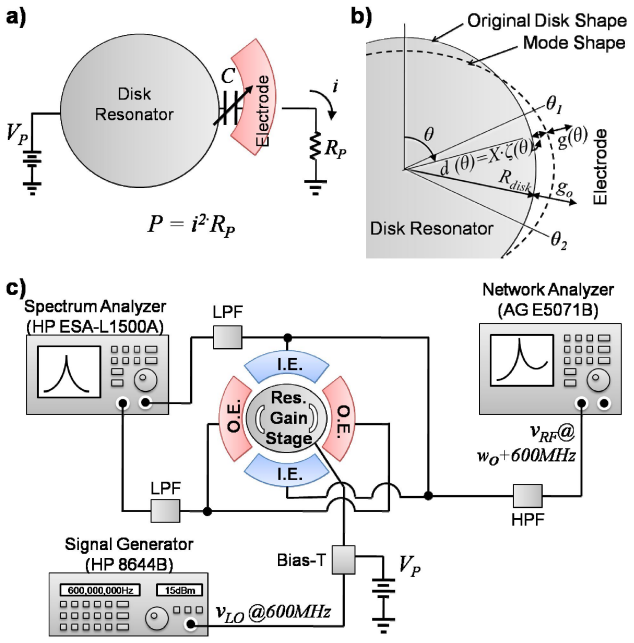

Figure 6: a) When a resonator vibrates, the gap between the resonator and the electrodes changes, resulting in current generation. b) Geometry schematic of a disk resonator. c) RF/LO mixing overtone test setup for simultaneous capacitive displacement measurement along each axis at resonance [7].

polysilicon surface micromachining process similar to those previously used [4]. Here, devices were patterned in a 3µm-thick polysilicon layer and electrodes were centered along the maximum displacement axes. A conformal sacrificial sidewall spacer high temperature oxide (HTO) deposition provided uniform lateral resonator-to-electrode gaps of 97nm. Slots were then patterned in the structure via a plasma etch. The devices were then released using hydrofluoric acid wet etching followed by critical point drying. SEM images of the fabricated devices are shown in Figure 5.

Capacitive Displacement Measurement

Determining the displacement gains in actual devices requires an ability to simultaneously measure and compare displacements along the different axes of a given device. Since the devices used here are capacitively transduced, displacements are most conveniently measured by measuring the currents generated by the charged time-varying capacitors between the disks and their electrodes (Figure 6a). Using the normalized radial displacement ζ of a disk resonator operating in its wine-glass mode in Figure 3 and the amplitude of oscillation X, the current generated at an electrode i is

$$i = V_P \frac{dC}{dt} = X \frac{\varepsilon_o h R_{disk} V_P \omega_o}{g_o^2} \int_{\theta_1}^{\theta_2} \zeta d\theta \qquad (1)$$

where, ε_o is the air permittivity, h is the disk thickness, ω_o is the angular resonant frequency, g_o is the static gap spacing, V_P is the bias voltage, R_{disk} is the disk radius, and θ_1 (overlap starts) and θ_2 (overlap finishes) are the overlap angles in Figure 6b.

By measuring the output power P at the electrode, the oscillation amplitude X can be obtained as

$$X = \sqrt{\frac{P}{R_P}} \frac{g_o^2}{\varepsilon_o h R_{disk} V_P \omega_o \cdot \int_{\theta_1}^{\theta_2} \zeta d\theta} \qquad (2)$$

where R_p represents parasitic interconnect resistance. Given this, the displacement d at resonance at a given location θ is governed by

$$d(\theta) = X \cdot \zeta(\theta) = \sqrt{\frac{P}{R_P}} \frac{g_o^2 \cdot \zeta(\theta)}{\varepsilon_o h R_{disk} V_P \omega_o \cdot \int_{\theta_1}^{\theta_2} \zeta d\theta} \qquad (3)$$

RF/LO Overtone Measurement

The output powers generated at the electrodes along each axis of each vibrating resonator under test were measured using the RF/LO overtone measurement setup illustrated in Figure 6c [7]. Using this setup, the motion of the resonator can be measured without interference from currents feeding through the static capacitors between the resonant structure and its electrodes. Here, a signal generator supplies an LO signal at 600MHz (which is away from the disk's resonance frequency) to the bias port via a bias-T, while a network analyzer provides an RF signal (with a frequency offset by ω_o from the LO signal). When this offset frequency, ω_o, matches the resonance frequency of the resonator, a force at ω_o is generated via the square-law voltage-to-force transfer function of the capacitive transducer that then drives the disk to resonance

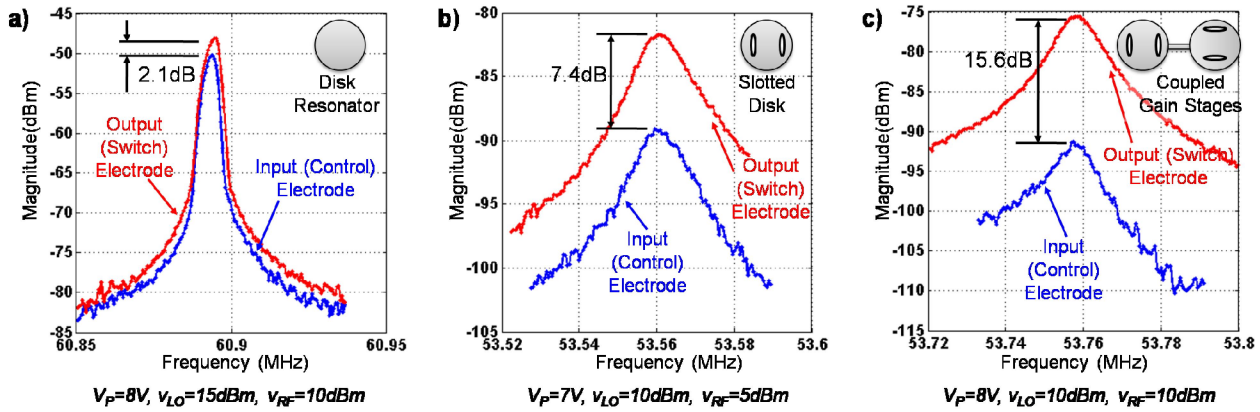

Figure 7: Comparison of measured power at each electrode of each resonator design using the RF/LO overtone measurement setup in Figure 6. The displacement along each axis can be extracted from the measured current out of each electrode. a) A conventional wine-glass mode disk resonator, b) Single resonant gain stage (slotted disk), c) Cascade of two slotted disk gain stages. The conventional disk resonator had virtually the same power generation within the measurement error range, while the single gain stage and two cascaded gain stages had significant differences.

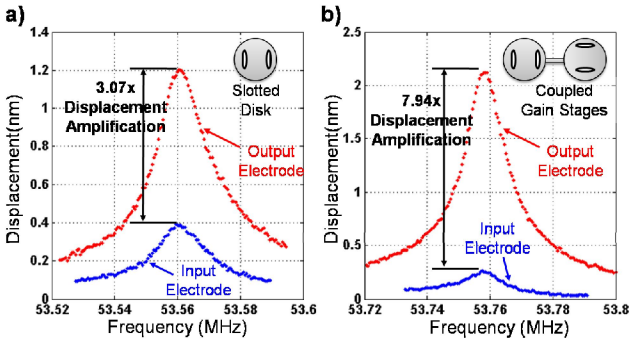

Figure 8: Comparison of displacement along each axis of displacement gain stages. These displacement data were extracted from Figure 7 using equation (3). a) The slotted disk resonator exhibited input and output axis displacements of 0.39nm and 1.20nm, respectively, providing an overall input-to-output displacement gain of 3.07x. b) In the case of two cascaded gain stages, the displacement was amplified by 7.94x, from 0.26nm (input) to 2.12nm (output).

vibration. Since the applied LO and RF signals do not coincide with the disk's resonance frequency, their feedthrough currents will not interfere with motional currents to be measured at resonance, allowing clean and accurate measurement by a spectrum analyzer.

Figure 7 shows the measured output power at each electrode for different designs. For the case of the conventional disk resonator, the measured power between the input and output electrodes were virtually identical, differing by less than the measurement error range. In contrast, significant differences are evident for the single resonant gain stage (slotted disk) and the cascaded two slotted disk gain stages.

Measured Displacement Gain

The displacement along each axis was extracted by plugging the resonator parameters (h=3µm, R_{disk}=32µm, g_o=97nm, and R_p=1.7kΩ) and the measured output power data (in Figure 7) into equation (3). Figure 8 plots the calculated displacements of each design. At resonance, the slotted disk (Figure 8a) exhibited input and output axis displacements of 0.39nm and 1.20nm, respectively, providing an input-to-output displacement amplification of 3.07x. The two cascaded gain stages (Figure 8b) exhibited an overall displacement gain of 7.94x, from 0.26nm (input) to 2.12nm (output). These displacement amplifications match well with the predictions of the ANSYS finite element analysis shown in Figure 2b and Figure 4b.

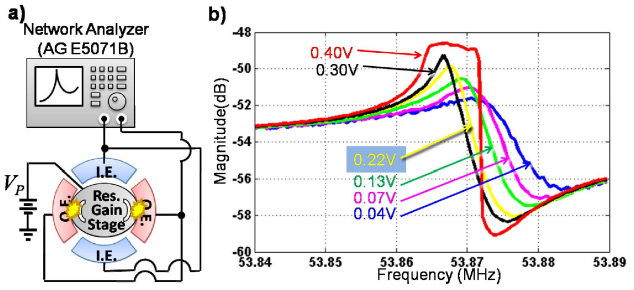

Figure 9: a) Test setup for switch-mode operation of resonant displacement gain stages. b) Frequency response plot of a preliminary resoswitch test of a single mechanical gain stage with V_{bias}=10V. The gain stage impacted the output electrodes and flattened the passband at V_{ac}=400mV.

Switch-Mode Operation of Displacement Gain Stages

To demonstrate the efficacy of displacement gain in resonant switch applications, a single resonant displacement gain stage (slotted disk) was tested in switch mode operation, as shown in Figure ***9***. Here, as the amplitude of the input voltage increases, the frequency response eventually flattens, indicating switching (impacting) of the resonant disk to the output electrode. This occurs when the input voltage amplitude is only 400mV$_{p\text{-}p}$, which is 6x smaller than for previous resoswitches without displacement gain [2, 3].

CONCLUSIONS

By strategic introduction of slots into their structures, the stiffnesses of disk resonators have been directionally engineered to yield more than 3x of displacement amplification from one axis to an orthogonal axis, and up to 7.94x when emplaced in two-stage cascades. Such gains have already led to 6x reductions in resoswitch actuation voltage. However, to truly reap the benefits of gain-enhanced resoswitches, further research is needed to lower their series resistance, e.g., by implementing them in metal (rather than polysilicon); and to improve their cycle lifetimes, where extensions from the current 16.5 trillion cycles to quadrillions of cycles are needed if such devices are to be used for practical power amplifier and power converter applications. Research on these topics is ongoing.

ACKNOWLEGEMENTS

The authors greatly appreciate the help and support of Li-Wen Hung, Inkyu Park, Hyuck Chou, and Matthew Wasilik from U.C.Berkeley for fabrication help and SEM image capture. This work was supported by DARPA.

REFERENCES

[1] P. D. Grant, et al., "A comparison between RF MEMS switches and semiconductor switches," in *ICMENS* 2004, pp. 515-521.

[2] Y. Lin, et al., "The micromechanical resonant switch ("Resoswitch")," in Hilton Head 2008, pp. 40-43.

[3] Y. Lin, et al., "A resonance dynamical approach to faster, more reliable micromechanical Switches," in *IEEE Frequency Control Symposium* Honolulu, Hawaii, USA, 2008, pp. 640-645.

[4] Y.-W. Lin, et al., "Series-resonant VHF micromechanical resonator reference oscillators," in *IEEE Journal of Solid-State Circuits*, vol. 39, pp. 2477-2491, 2004.

[5] S.-S. Li, et al., "Disk-array design for suppression of unwanted modes in micromechanical composite-array filters," in *IEEE MEMS'06*, Istanbul, Turkey, 2006, pp. 866-869.

[6] Y.-W. Lin, et al., "Low phase noise array-composite micromechanical wine-glass disk oscillator," in *IEDM 2005*, pp. 287-290.

[7] J. R. Clark, et al., "High-Q UHF micromechanical radial-contour mode disk resonators," in *IEEE Journal of Microelectromechanical Systems*, vol. 14, pp. 1298-1310.